Edward R. T. Tiekink and Julio Zukerman-Schpector

14 Solute–solvent interactions mediated by main group element(lone-pair)···π(aryl) interactions

14.1 Introduction

Since the disclosure of tellurium(II, IV)···π(aryl) interactions in their crystal structures [1], there has been increasing interest in ascertaining the importance of this type of supramolecular synthon, i.e. main group element(lp)···π(arene), in the structural chemistry of main group element chemistry [2–10]. It is noted in passing that analogous interactions have been revealed in structural biology and are known to provide important stabilising contacts [11, 12]. In molecular structural chemistry, the emphasis thus far has been upon seeking "stand-alone" element(lp)···π(arene) contacts and determining the supramolecular architectures they sustain [2–10]. Usually these architectures are zero- and one-dimensional; however, examples of two- and even three-dimensional aggregation patterns are known [9, 10]. With the restriction that the element(lp)···π(arene) interaction operates in a given dimension within a crystal, in isolation from other supramolecular synthons, these interactions occur in a maximum of 14% of thallium(I) structures. This is reduced to 9% in bismuth(III) structures and down to a minimum of 2–3% for tin(II) and lead(II) compounds [9, 10]. In terms of bonding, it is likely that the lone-pair···π interaction has similar features to halogen bonding [13] in that there is an asymmetric distribution of electron density in the lone-pair of electrons. This leaves an electropositive region at the tip of the lone-pair that interacts with the π electrons of the ring. This electron-deficient region is termed variously a σ-hole or polar cap, and the energy of stabilisation imparted by these interactions is in the region of $10\,kJ\,mol^{-1}$, i.e. similar to that imparted by C–H···π(aryl) interactions. In keeping with the theme of the present volume, "*Aspects of Multi-Component Crystals: Synthesis, Concepts and Function*", a description herein of the supramolecular architectures sustained by main group element(lp)···π(aryl) interactions is given where the π system is a solvent molecule such as benzene.

14.2 Procedures

Standard protocols were utilised to identify structures for the current survey [10]. The Cambridge Structural Database (CSD: version 5.37 + 2 updates) [14] was searched using CONQUEST (version 1.18) [15]. There were two key geometric restraints, as illustrated in Figure 14.1a. The first restraint is the distance d, between the metal centre and the ring centroid, labelled Cg, which was set at 4.0 Å. This distance is shown to be suffi-
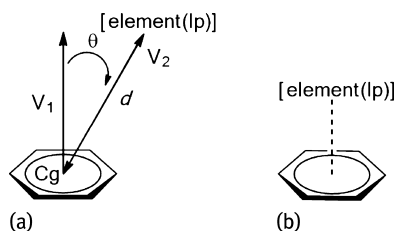
Fig. 14.1: (a) The geometric restrictions employed to identify element(lp)···π(arene) interactions. The distance d (Å) is the separation between the ring centroid, Cg, and the element. The angle θ (°) is between the normal to the arene ring, V_1, and the vector, V_2, between the ring centroid and the element. (b) A representation of a delocalised element(lp)···π(arene) interaction where the element's lone-pair interacts approximately equally with all six carbon atoms of the aryl ring.

cient to identify relevant contacts [10]. The second restraint is the angle θ, which is the angle between the normal to the plane through the aryl ring (V_1) and the vector from Cg to the main group element (V_2). This angle indicates the relative location of the element above the C_6 plane and was restricted to $\leq 20°$, so that only "delocalised" [16] element(lp)···π(aryl) interactions were retrieved. The consequence of this restriction is that the lp···C separations are approximately equal (Figure 14.1b). This restriction removes "localised" interactions where the lone-pair is orientated towards a single atom of the aryl ring only as well as "semi-localised" interactions where the lone-pair is engaged with only one of the bonds of the ring [16]. The only other restrictions that were applied were those structures with unresolvable disorders, which were omitted. Furthermore, structures determined from powder data were not included. This resulted in 37 "hits" satisfying the specified criteria. Each data set, in the form of a common interface file, was manually scrutinised and analysed quantitatively using PLATON [17]. Diagrams are original and were drawn using DIAMOND [18].

14.3 Discussion

Structures are discussed starting from the gallium-group elements with benzene, followed by examining the substituted forms of the C_6 ring. The tin group elements are described. Within each group, mononuclear species are discussed before binuclear species. Finally, for each sub-category, lower nuclearity aggregates are described before higher nuclearity aggregates.

The chemical diagrams were generated in ChemDraw® and show only the interacting species. As such, other species in the crystal, such as counter ions, are not illustrated. In the diagrams showing aggregation patterns, all hydrogen atoms have been omitted for reasons of clarity. The arene rings forming the element(lp)···π(arene) interactions are highlighted in purple. The interaction is indicated by a dashed purple line.

14.3.1 Group III

Only thallium(I) compounds have been found to form Tl(lp)···π(arene) interactions where the arene ring is a solvent molecule. There are six examples, (1)–(6), and their chemical diagrams are shown in Figure 14.2.

The first three structures in this category are mononuclear thallium(I) compounds. In (1), a molecule of mononuclear {bis[3-(9-triptycyl)pyrazolyl]hydroborato} thallium(I) [19] associates with a solvent toluene molecule via a Tl(lp)···π(toluene) interaction [d = 3.22 Å and θ = 3.7°] to form a zero-dimensional aggregate in which the thallium(I) atom increases its coordination number from 2 (N_2 donor set) to 3 within a distorted trigonal planar geometry (Figure 14.3a). A similar aggregation pattern is
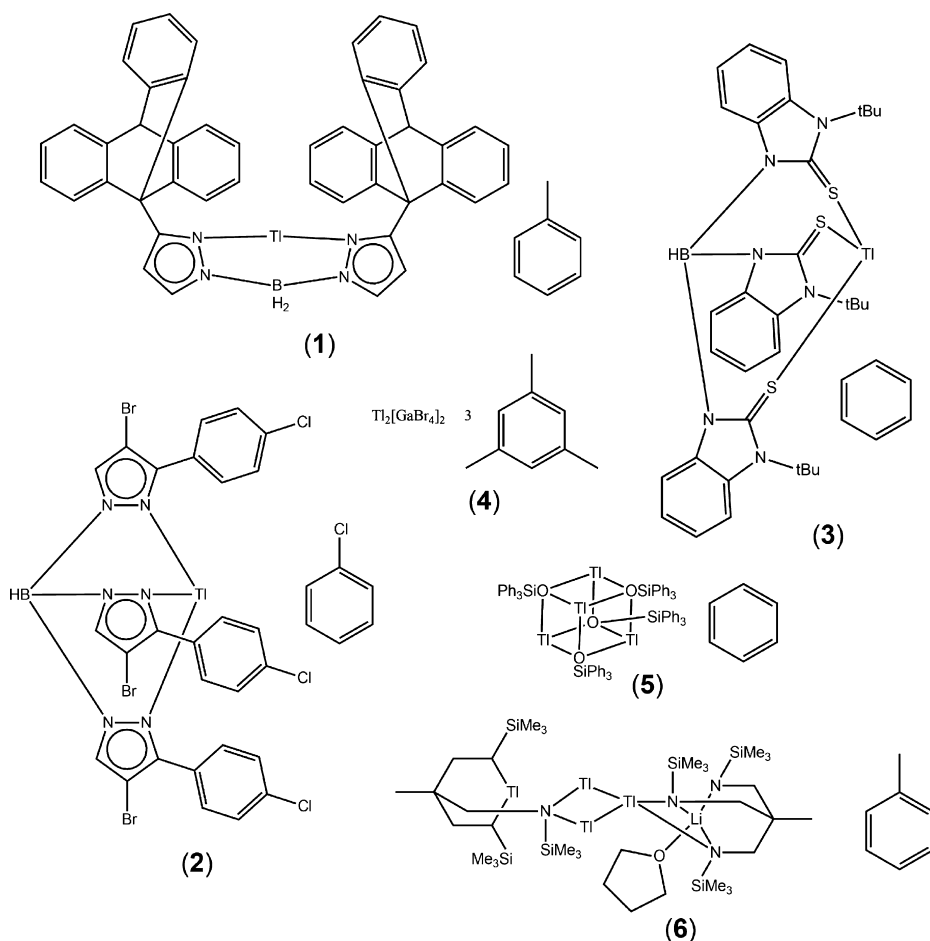

Fig. 14.2: Chemical diagrams for (1)–(6). In this and subsequent figures showing chemical diagrams, only species participating in element(lp)...π(arene) interactions are shown.
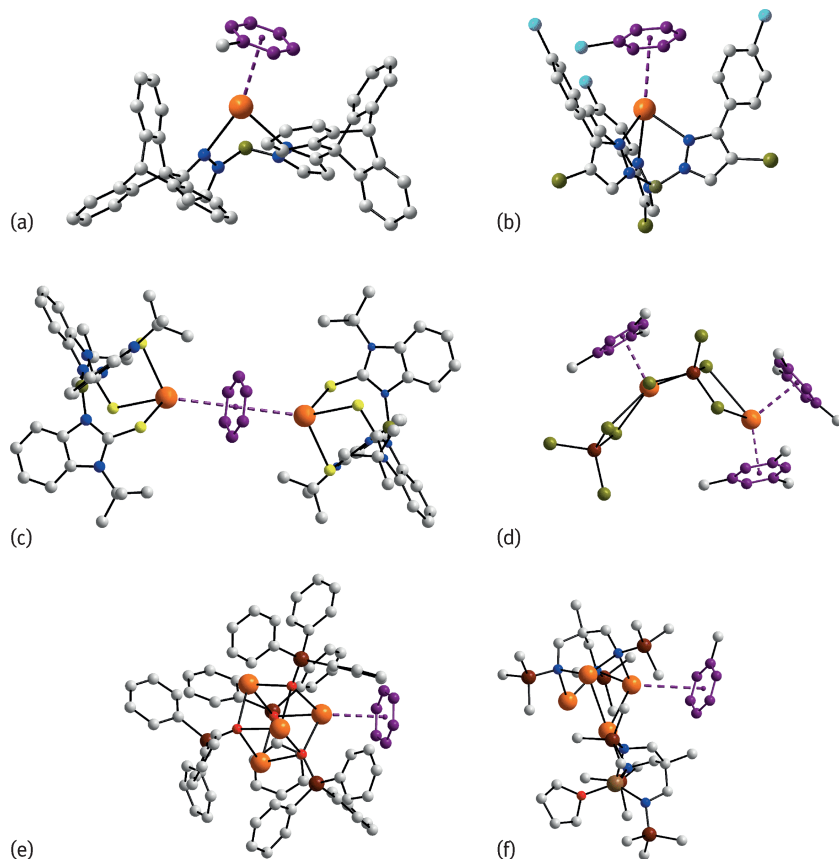
Fig. 14.3: Supramolecular aggregation via Tl(lp)···π(arene) interactions in the crystal structures of (1)–(6) shown in (a)–(f), respectively. Colour code: Tl (or other main group element), *orange*; bromide, *olive green*; chloride, *cyan*; sulphur, *yellow*; silicon, *brown*; oxygen, *red*; nitrogen, *blue*; boron, *grey green*; and lithium, *beige*.

found in (2), whereby a single Tl(lp)···π(chlorobenzene) interaction [d = 3.69 Å and θ = 14.5°] is found in (hydrogen tris(4-bromo-3-(p-chlorophenyl)pyrazolyl)borato) thallium(I) chlorobenzene solvate [20] to give a two-molecule, zero-dimensional aggregate (Figure 14.3b). The thallium(I) centre in bis(hydrogen tris(2-thioxo-3-t-butylbenzimidazol-1-yl)borate)thallium(I) (3) [21] is located on a three-fold axis of symmetry and was characterised crystallographically as its hemi-benzene solvate. From symmetry, the benzene ring accepts two Tl(lp)···π(toluene) interactions [d = 3.39 Å and θ = 0.0°] to form a binuclear three-molecule aggregate (Figure 14.3c). The original coordination geometry for each thallium atom was pyramidal, defined by a S_3 donor set. The coordination geometry is expanded to four with the interaction of the benzene ring.

In binuclear di-thallium(I) bis[tetrabromo-gallium(III)] tris(1,3,5-trimethylbenzene) solvate (4) [22] one [GaBr$_4$]$^-$ anion bridges two thallium(I) centres, whereas the other is terminally bound, giving two independent thallium centres, each of which is associated with 1,3,5-trimethylbenzene molecules. The thallium forming four Tl···Br bonds is connected to one 1,3,5-trimethylbenzene molecule [$d = 2.94$ Å, $\alpha = 2.9°$] whereas the other coordinatively unsaturated thallium(I) atom is connected to two 1,3,5-trimethylbenzene molecules [$d = 3.01$ Å, $\alpha = 5.4°$; $d = 3.03$ Å, $\alpha = 3.1°$]. The result is a binuclear, zero-dimensional aggregate (Figure 14.3d). In tetranuclear tetrakis(μ_3-triphenylsilanolato)-tetra-thallium(I) benzene solvate (5) [23] only one of the four thallium(I) centres forms a single Tl(lp)...π(benzene) interaction [$d = 3.20$ Å and $\theta = 2.7°$] to form a tetranuclear, two-molecule and zero-dimensional aggregate (Figure 14.3e). In the same way, a single Tl(lp)···π(toluene) interaction [$d = 3.20$ Å and $\theta = 2.7°$] is found in the structure of tetranuclear (μ_3-1,1,1-tris(trimethylsilylamido)ethane)(μ_3-1,1-bis(trimethylsilylamido)-1-(trimethylsilylamino)ethane)-tetrahydrofuran-tetra-thallium(I)-lithium toluene solvate (6) (Figure 14.3f) [24].

14.3.2 Group IV

14.3.2.1 Tin(II)

Three tin(II) structures, (7)–(9), have been revealed to feature Sn(lp)···π(arene) interactions in their crystal structures. Chemical diagrams for these are shown in Figure 14.4.

In the binuclear structure of bis(μ_2-2,6-dimethylphenolato)-bis(2,6-dimethylphenolato)-di-tin(II).2(toluene) (7) [25], two centrosymmetrically related molecules associate via Sn(lp)···π(aryl) interactions [$d = 3.36$ Å and $\theta = 10.8°$] to form a dimeric, zero-dimensional aggregate. Toluene molecules interact with the terminal tin atoms [$d = 3.59$ Å and $\theta = 7.6°$] so that each Sn(II) atom in (7) forms a single Sn(lp)···π(aryl) interaction and adopts a pseudo-tetrahedral geometry. In mononuclear 2,3-bis(trimethylsilyl)-1-stanna-2,3-dicarba-closoheptaborane(4) hemi-benzene solvate (8) [26], the tin(II) centre is coordinated by three boron and two carbon atoms, but in a way that leaves the tin(II) atom exposed. This enables the formation of a Sn(lp)···π(benzene) contact [$d = 3.73$ Å and $\theta = 13.6°$] and, as the benzene molecule of solvation is located about a centre of inversion, a binuclear three-molecule aggregate ensues. The tetranuclear cluster molecule, bis(μ_3-oxo)-octakis(μ-trifluoroacetato)-di-tin(II)-di-tin(IV), is disposed about a centre of inversion and is crystallised as a benzene solvate, also located about a centre of inversion, with the ratio between molecules being 1:1 (9) [27]. The exocyclic tin atoms, i.e. being tin(II) as opposed to the endocyclic tin(IV) atoms and having square-pyramidal geometries defined by five oxygen atoms, form Sn(lp)···π(benzene) contacts [$d = 3.32$ Å and $\theta = 6.1°$] to generate a supramolecular chain with a flattened step topology.
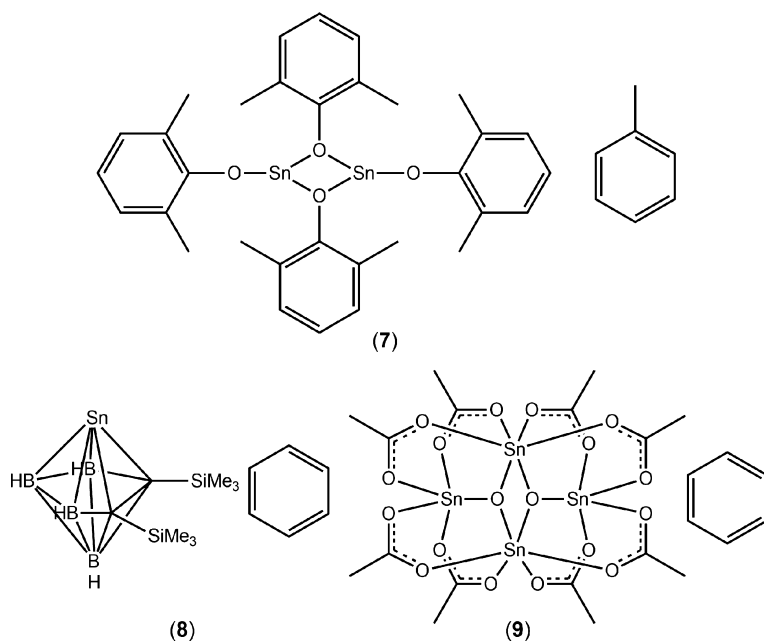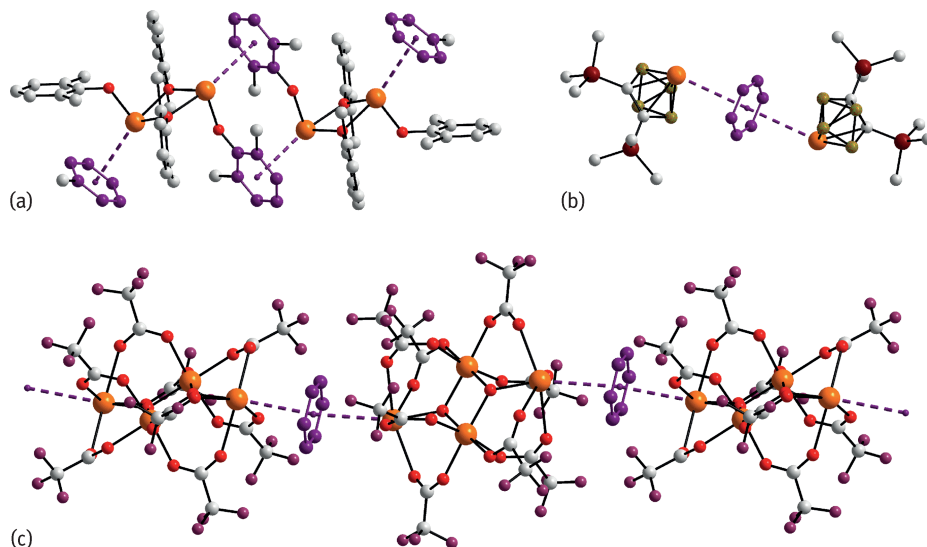
Fig. 14.4: Chemical diagrams for (7)–(9).

Fig. 14.5: Supramolecular aggregation via Sn(lp)...π(arene) interactions in the crystal structures of (7)–(9), shown in (a)–(c) respectively. Additional colour code: fluoride, *violet red*.

14.3.2.2 Lead(II)

Five lead(II) structures, (10)–(14), feature at least one Pb(lp)···π(arene) interaction in their crystal structures. See Figure 14.6 for chemical diagrams.

The first three structures in this category are mononuclear, with each lead(II) centre forming a single Pb(lp)···π(arene) contact. Thus, the lead(II) atom in (10), i.e. bis(diphenylpentane-2,4-diiminato)lead(II) toluene solvate [28], is coordinated by four nitrogen atoms, but there is a large void above the lead(II) atom (Figure 14.7a), which is occupied by the toluene molecule [d = 3.66 Å and θ = 8.6°]. A relatively high coordination number is also found in (11), bis(2,4,6,8-tetra-t-butyl-1-oxo-1H-phenoxazin-9-olato)lead(II) benzene di-solvate [29], where the lead(II) is in a N_2O_4 donor set. However, once again, there is a large void to accommodate one of the two benzene molecules co-crystallised with the lead compound via a Pb(II)···π(benzene) interaction [d = 3.77 Å and θ = 17.9°] (Figure 14.7b). The mononuclear structure of 2,3-bis(trimethylsilyl)-2,3-dicarba-1-plumba-closo-heptaborane(6) benzene solvate

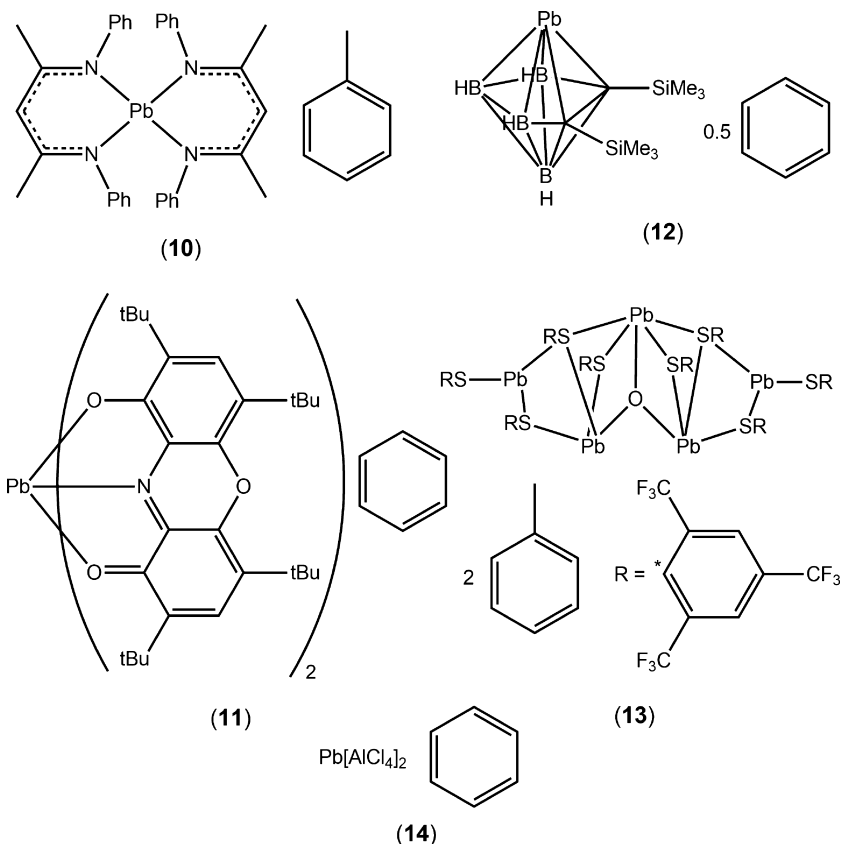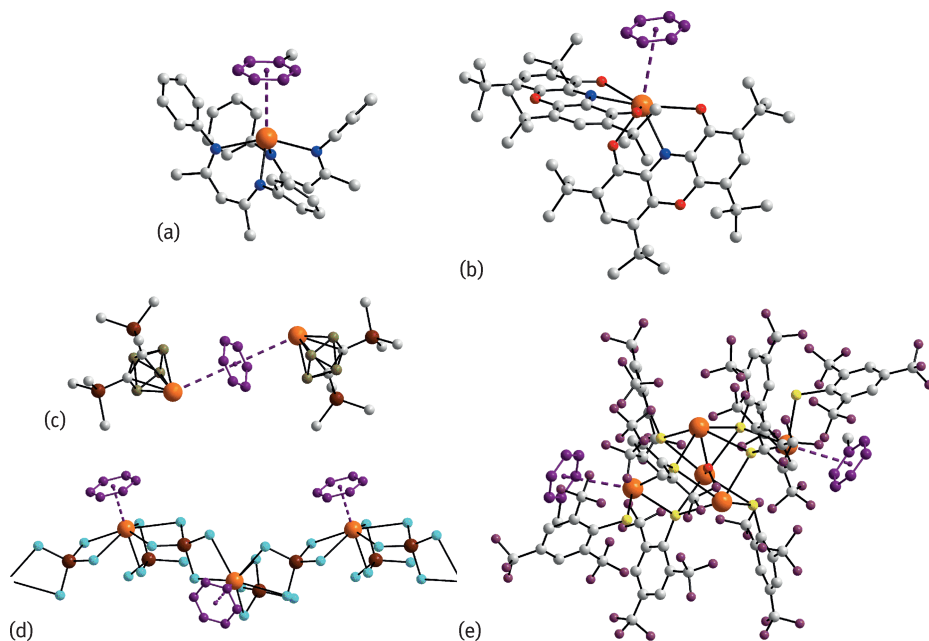**Fig. 14.6:** Chemical diagrams for (10)–(14).

Fig. 14.7: Supramolecular aggregation via Pb(lp)...π(arene) interactions in the crystal structures of (10)–(14) shown in (a)–(e), respectively. Additional colour code: aluminium, *brown*.

(12) [30] is isostructural with (8) (Figure 14.5b) [26]. Thus, the lead(II) centre is coordinated by a B_3C_2 donor set, but the atoms comprising the cluster lie to one side of the molecule, enabling the formation of a Pb(lp)···π(benzene) contact [d = 3.74 Å and θ = 16.9°] with a centrosymmetric benzene molecule, which results in a binuclear, three-molecule aggregate (Figure 14.7c).

Two of the five lead(II) atoms in pentanuclear bis(μ_3-2,4,6-tris(trifluoromethyl) phenylthiolato)-(μ_3-oxo)-tetrakis(μ_2-2,4,6-tris(trifluoromethyl)phenylthiolato)-bis(2,4,6-tris(trifluoromethyl)phenylthiolato)-penta-lead(II), isolated as a 1:2 toluene solvate (13) [31] forms Pb(lp)···π(arene) interactions [d = 3.55 Å and θ = 19.1°; d = 3.70 Å and θ = 17.8°] (Figure 14.7d). The common feature of the two interacting lead(II) atoms is that they exist in pyramidal coordination geometries, defined by S_3 donor sets, exposing the lone-pair to the rings. By contrast, the remaining lead atoms have higher coordination numbers, i.e. 4 and 5.

[Lead(II) bis(tetrachloridoaluminium(IV))]$_n$ (14) [32] is a coordination polymer that was isolated as a benzene solvate, with the ratio between lead atoms and solvent molecules being 1:1, enabling each lead atom to form a Pb(lp)···π(arene) contact [d = 2.78 Å and θ = 1.1°]. As seen from Figure 14.7e, each lead atom, despite being coordinated by six chlorido atoms, is in a distorted pentagonal-bipyramidal coordination geometry with the benzene ring lying to one side of the pentagonal plane.

14.3.3 Group V

14.3.3.1 Arsenic(III)

Three arsenic(III) solvates, (15)–(17), feature As(lp)···π(arene) interactions in their molecular packing. Chemical diagrams for these are shown in Figure 14.8.
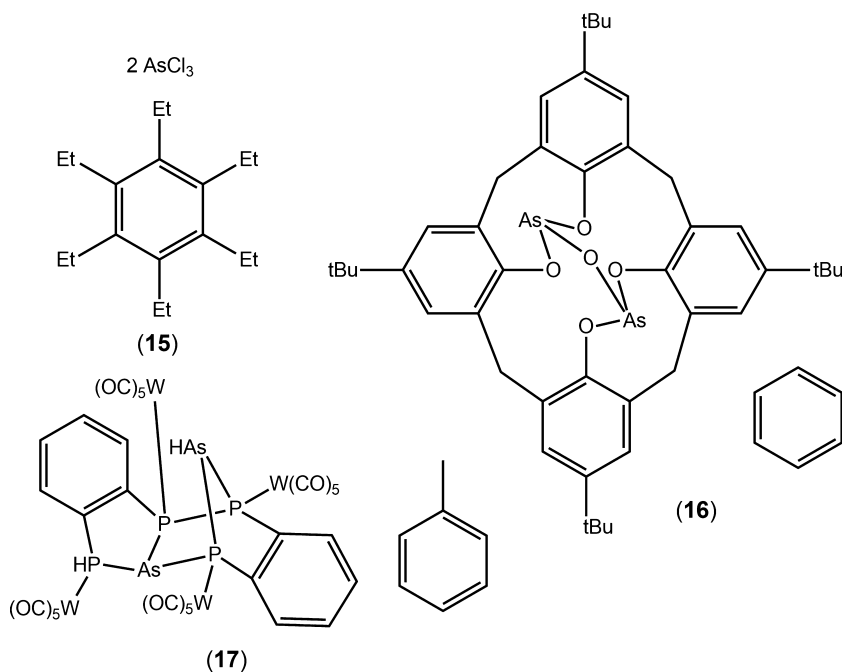

Fig. 14.8: Chemical diagrams for (15)–(17).

Each of the trichloroarsane arsenic(III) centres in bis[trichloroarsane(III)] hexaethylbenzene (15) [33] associates with the hexaethylbenzene ring via a As(lp)···π(arene) interaction [d = 3.14 Å and θ = 0.0°], with the entire three-molecule aggregate (Figure 14.9a) having crystallographic 3-fold symmetry. In (16), a binuclear compound, (μ_2-5,11,17,23-tetra-t-butylcalix(4)arene-25,26,27,28-tetraolato)-(μ_2-oxo)-di-arsenic(III) benzene solvate [34], both arsenic(III) atoms have three-coordinate, pyramidal geometries defined by an O_3 donor set, but only one centre forms a As(lp)···π(arene) interaction [d = 3.57 Å and θ = 3.6°] (Figure 14.9b).

In the heterometallic complex, (μ_4-7H-5,13-arsano(1,3,2)benzodiphospharsolo (1,2-b)(1,2,4,3)benzotriphospharinine)-icosacarbonyl-tetra-tungsten toluene solvate (17) [35], two distinct coordination environments are noted for arsenic(III). One is pyramidal and based on a P_3 donor set, whereas the other is also pyramidal, but based
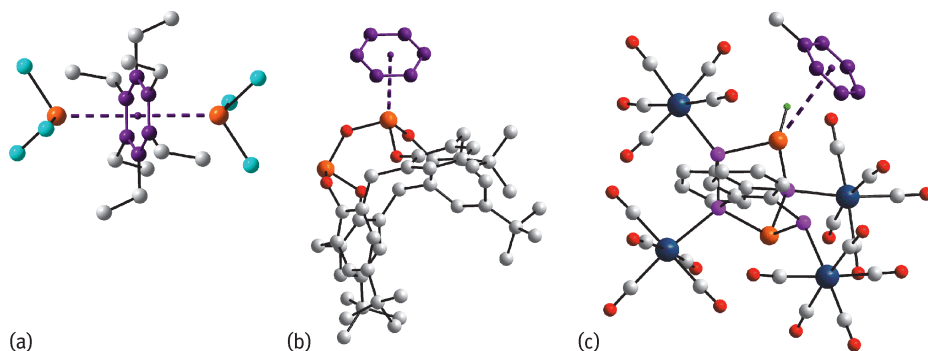
Fig. 14.9: Supramolecular aggregation via As(lp)…π(arene) interactions in the crystal structures of (15)–(17) shown in (a)–(c) respectively. Additional colour code: tungsten, *indigo*; phosphorous, *pink*; hydrogen, *green*.

on a HP$_2$ donor set. It is the latter that forms the As(lp)…π(arene) interaction leading to a two-molecule, zero-dimensional aggregate [d = 3.72 Å and $θ$ = 10.5°].

14.3.3.2 Antimony(III)

The first four structures in this category, (18)–(21), are examples of classic Menschutkin complexes [36, 37]. Chemical diagrams for these and for two further structures featuring Sb(lp)…π(arene) interactions in the crystal structures, (22) and (23), are shown in Figure 14.10. Although the common feature of (18)–(21) is the presence of mononuclear species, in trichlorido-antimony toluene (18) [38] and tribromidoantimony(III) mesitylene (19) [39] solvate a single interaction occurs between antimony(III) and the solvent molecule. In (18), there are two independent complex:solvent pairs and each of these forms a Sb(lp)…π(arene) interaction [d = 3.10 Å and $θ$ = 7.7°; d = 3.16 Å and $θ$ = 9.0°]. The structure of (19) is even more remarkable in that there are four independent pairs of molecules in the asymmetric unit, and each of these forms a Sb(lp)…π(arene) interaction [d = 3.22 Å and $θ$ = 8.8°; d = 3.22 Å and $θ$ = 9.4°; d = 3.30 Å and $θ$ = 5.3°; d = 3.33 Å and $θ$ = 5.0°]. One of these complex : solvent pairs is shown in Figure 14.11a. In each of bis(trichlorido-antimony) benzene solvate (20) [40] and bis[trichloridoantimony(III)] p-xylene solvate (21) [41], each solvent molecule forms two Sb(lp)…π(arene) interactions. The absence of symmetry in (20) (Figure 14.11b) implies two independent set of parameters [d = 3.25 Å and $θ$ = 7.6°; d = 3.33 Å and $θ$ = 7.4°] whereas the solvent in (21) lies about a centre of inversion [d = 3.14 Å and $θ$ = 11.5°].

The hexa-antimony(III) cluster complex constructed about a {SbO}$_6$ ladder, bis($μ$-diphenylsilanediolato)-bis($μ$-hydroxo)-hexakis($μ$-oxo)-octaphenyl-hexa-antimony(III), crystallises as a 1 : 1 toluene solvate (22) [42]. From the formulation and as illustrated in Figure 14.11c, only one Sb(lp)…π(arene) interaction is formed [d = 3.67 Å and $θ$ = 9.6°].
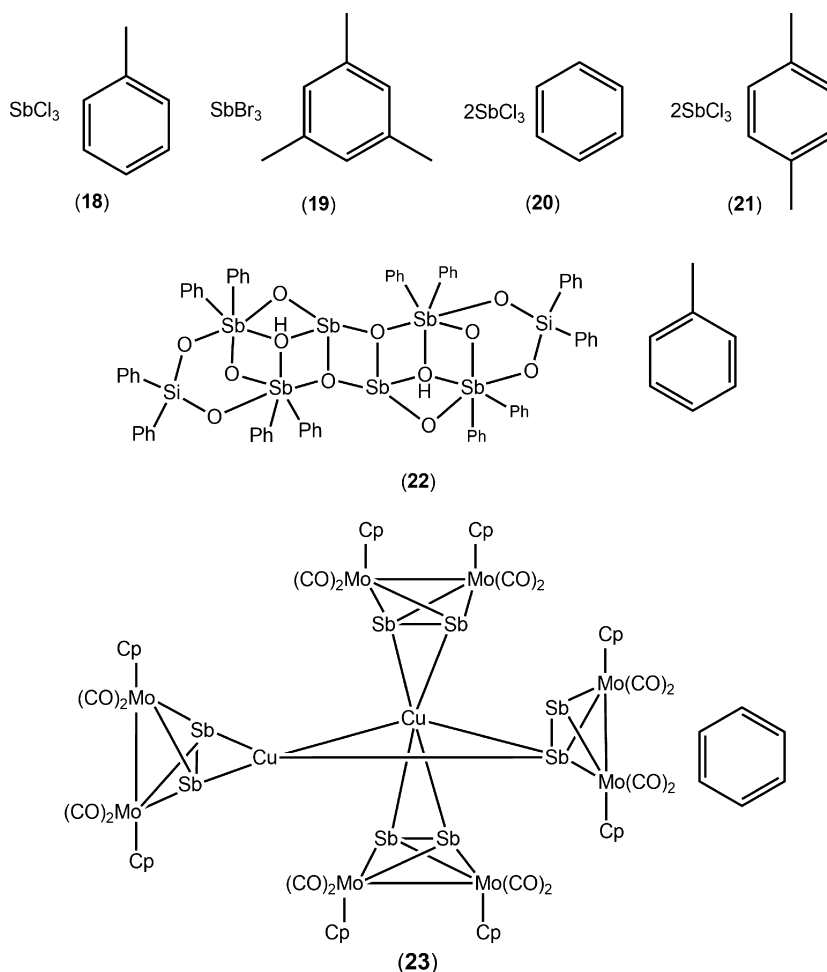
Fig. 14.10: Chemical diagrams for (18)–(23).

The final antimony(III) complex to be described is that of heterometallic and organo-metallic tris[μ_4-di-antimony(III)]-[μ_3-di-antimony(III)]-tetrakis(tetracarbonyl-bis(η^5-cyclopentadienyl))-di-copper(I)-octa-molybdenum(0) bis[tetra-chlorido-gallium(III)] benzene solvate (23) [43]. The antimony(III) atom that formally does not form an inter-action to a copper(I) atom forms the Sb(lp)···π(arene) contact with the solvent benzene molecule [d = 3.47 Å and θ = 1.6°] (Figure 14.11d).

14.3.3.3 Bismuth(III)

With nine structures featuring Bi(lp)···π(arene) interactions, bismuth(III) compounds are the most frequently represented in the present survey. The nuclearity of the spe-
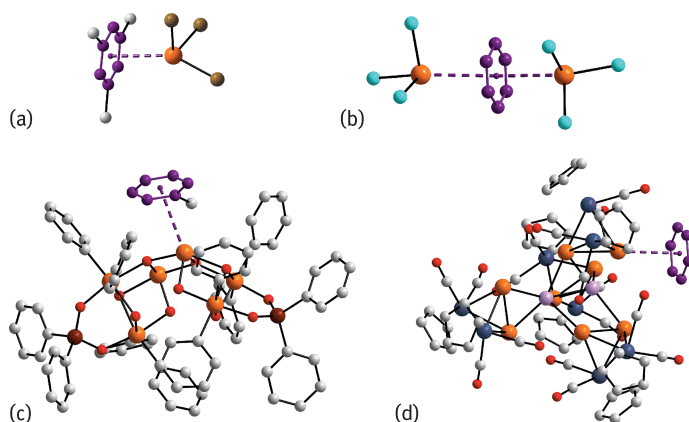
Fig. 14.11: Supramolecular aggregation via Sb(lp)…π(arene) interactions in the crystal structures of (19), (20), (22) and (23) shown in (a)–(d) respectively. Additional colour codes: molybdenum, *indigo*; copper, *mauve*.

cies ranges from 1 up to 14; therefore, a large number of distinct structural motifs are observed. The first three structures to be discussed, (24)–(27) (Figure 14.12) are formally mononuclear BiCl$_3$ and are typical Menschutkin complexes. Despite these similarities, three quite distinct structural motifs are observed in their crystal structures. In trichlorido-bismuth(III) toluene (24) [44] (Figure 14.13a), two independent molecules comprise the crystallographic asymmetric and each bismuth(III) centre forms a single Bi(lp)…π(arene) interaction to a toluene molecule [d = 3.04 Å and θ = 3.6°; d = 3.09 Å and θ = 7.9°]. In the other two structures, significant supramolecular association occurs, owing to strong Bi…Cl secondary bonding interactions. Thus, in catena[(bis(μ_2-chlorido))-chlorido-bismuth(III) (η^6-m-xylene)] (25) [45], a coordination polymer is observed (Figure 14.13b), decorated with m-xylene molecules held in place by Bi(lp)…π(arene) interactions [d = 2.99 Å and θ = 5.8°]. By contrast, an oligomeric aggregate is observed for bis(hexamethylbenzene) tetrakis(μ_2-chlorido)-octachloro-tetra-bismuth(III) (26) [36] (Figure 14.13c). The oligomer features four bismuth(III) centres and is disposed about a crystallographic four-fold inversion centre. The independent bismuth(III) atom associates with a hexamethylbenzene molecule [d = 3.07 Å and θ = 2.6°].

The next four structures to be described, (27)–(30) (Figure 14.12), are tetranuclear bismuth(III) compounds. In bis(μ_3-oxo)-tetrakis(μ_2-1,1,1,3,3,3-hexafluoro-2-propoxo)-tetrakis(1,1,1,3,3,3-hexafluoro-2-propoxy)-tetra-bismuth(III) toluene solvate (27) [46], the cluster is situated about a centre of inversion. There are two distinct coordination environments for bismuth(III): the endocyclic atoms based on a O$_5$ donor set and the exocyclic bismuth(III) atoms, which are coordinated within a O$_4$ donor set. It is one exocyclic bismuth(III) atoms that form the Bi(lp)…π(arene) interactions [d = 3.56 Å and θ = 15.5°] leading to distorted trigonal bipyramidal geo-
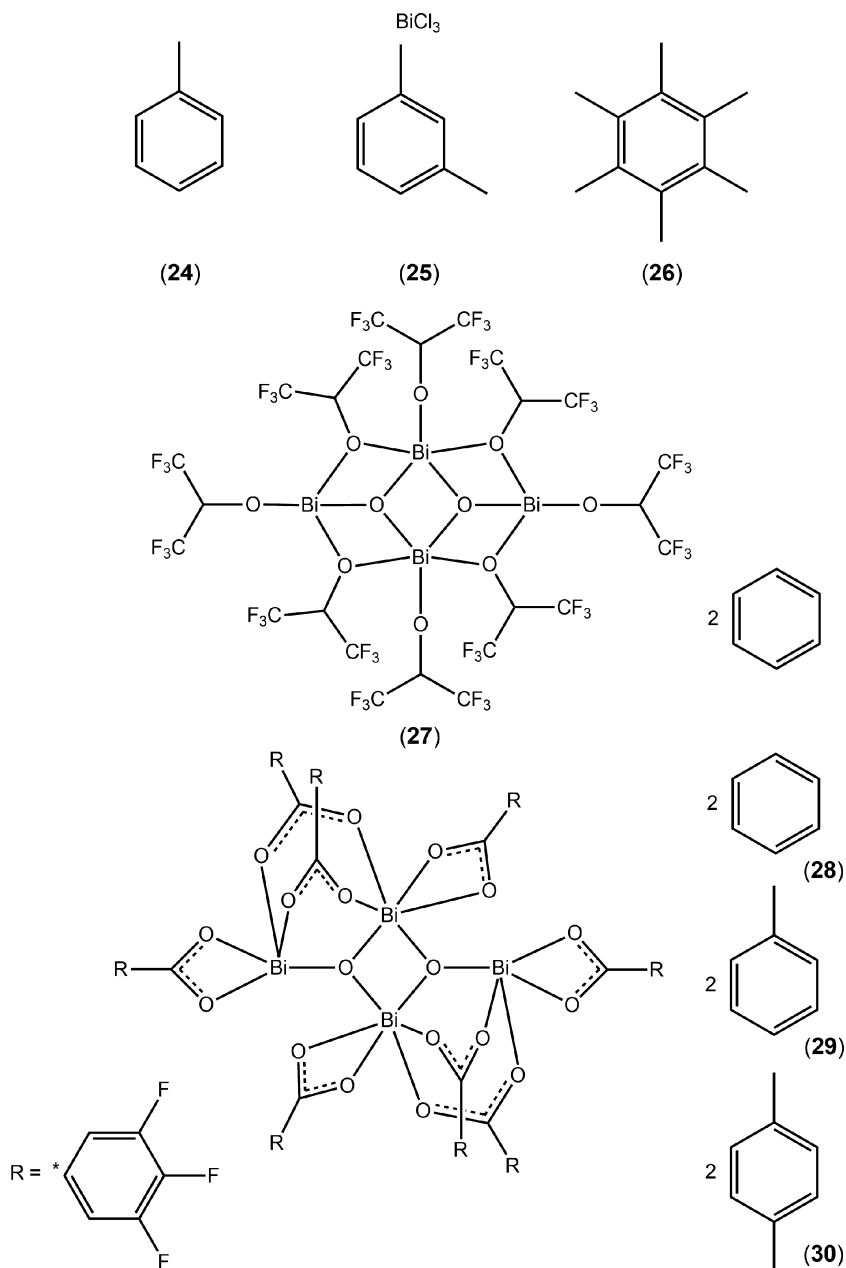
Fig. 14.12: Chemical diagrams for (24)–(30).

metries (Figure 14.13d). There are three tetranuclear structures that differ only in the pattern of fluoride substitution in the benzoate anions. These are exemplified in Figure 14.13e by bis(μ_3-oxo)-octakis(μ_2-3,4,5-trifluorobenzoato)-tetra-bismuth(III),
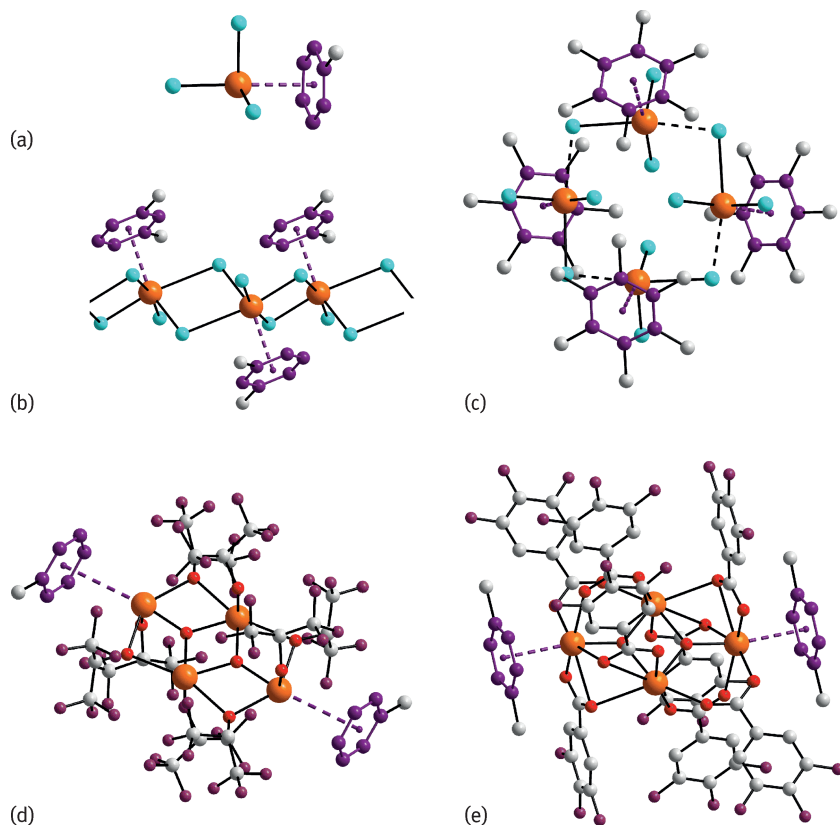
Fig. 14.13: Supramolecular aggregation via Bi(lp)…π(arene) interactions in the crystal structures of (24)–(28) shown in (a)–(e) respectively.

characterised as a 1,4-dimethylbenzene disolvate (28) [47]. The centrosymmetric molecular framework of the cluster may also be described as comprising endocyclic and exocyclic bismuth(III) atoms. The coordination numbers here, each based on donor sets provided by oxygen atoms, are 7 and 6 respectively. The exocyclic bismuth(III) centres form the Bi(lp)···π(arene) interactions [d = 3.13 Å and θ = 5.6°], leading to distorted pentagonal bipyramidal geometries. Very similar structures and modes of association with solvent are found in both (29), i.e. having benzene rather than 1,4-dimethylbenzene as the solvent [d = 3.02 Å and θ = 3.4°] [47], and (30) having toluene as the solvent [d = 3.13 Å and θ = 2.7°] [48].

The molecular structures of (31) and (32) contain 8 and 14 bismuth(III) atoms respectively (Figure 14.14). Compound (31) has composition bis(μ_4-5,11,17,23,29,35,41,47-octa-t-butyl-49,50,51,52,53,54,55,56-octaoxycalix(8)arene)-tetrakis(μ_4-oxo)-octa-bismuth(III) acetonitrile diethyl ether toluene solvate [49]. The cluster is disposed about a four-fold inversion centre. There are two independent bismuth(III) atoms and each

(31)

$[Bi_{14}(\mu\text{-O})_{10}(\mu_4\text{-O}_2P(=O)tBu)_6(\mu_3\text{-O}_2P(=O)tBu)_4(\mu_4\text{-O}_2P(OH)tBu)_2].6C_6H_6$
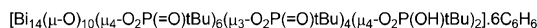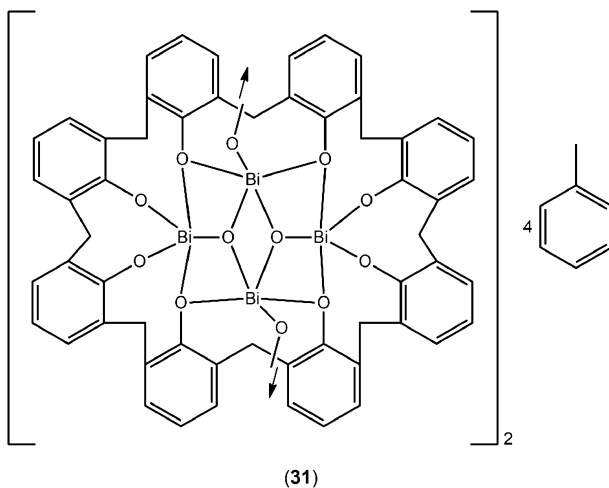
(32)

Fig. 14.14: Chemical diagrams for (31) and (32).

exists within a five-coordinate geometry defined by oxygen atoms. One of these associates with a toluene molecule [d = 3.51 Å and θ = 6.4°], leading to a heavily distorted octahedral geometry (Figure 14.15a).

The final bismuth(III) structure, revealed to possess Bi(lp)···π(arene) interactions, is that of hexakis(μ_4-t-butylphosphonato)-bis(μ_4-t-butylhydrogenphosphonato)-decakis(μ_3-oxo)-tetrakis(μ_3-t-butylphosphonato)-tetradeca-bismuth(III) benzene solvate tetrahydrate (32) [50]. There is a high degree of crystallographic symmetry in the compound, and both the cluster and benzene molecules have *mmm* symmetry. Six of the 14 bismuth(III) centres associate with benzene molecules, because there are two independent interactions [d = 3.19 Å and θ = 0.0°; d = 3.21 Å and θ = 5.8°]. Four of the interactions are terminal, but two are bridging, leading to the formation of a linear supramolecular chain (Figure 14.15b).

14.3.4 Group VI

14.3.4.1 Selenium(II)

The two main oxidation states for selenium in their molecular compounds are +IV and, especially, +II leading to, one and two lone-pairs of electrons respectively. The element in both oxidation states has been shown to form Se(lp)···π(arene) interactions in the crystal structures of its molecular compounds [7, 8]. When the accepting π-system is
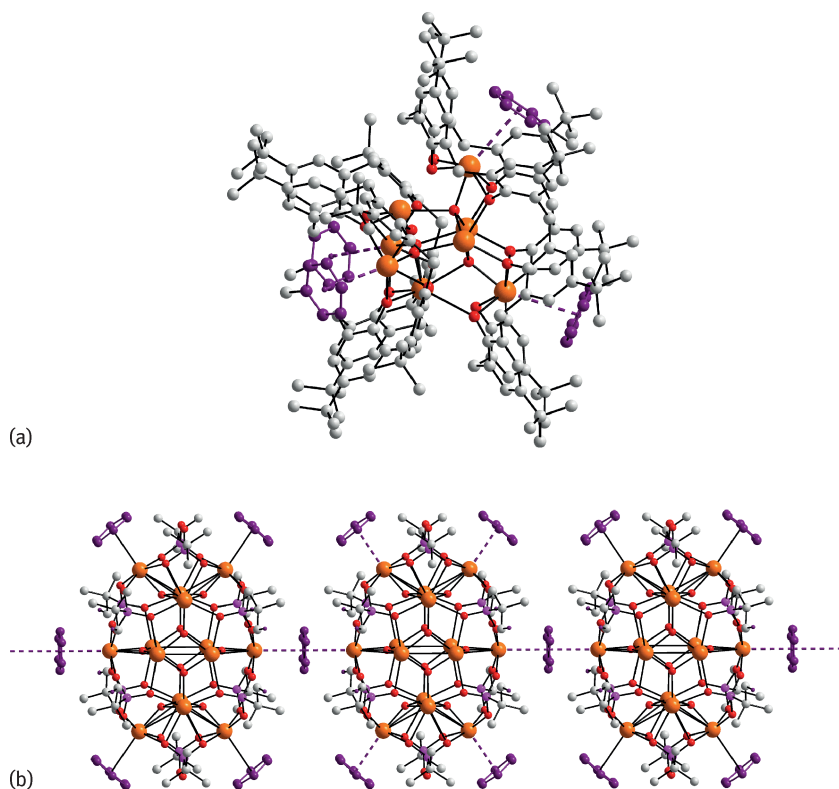
(a)

(b)

Fig. 14.15: Supramolecular aggregation via Bi(lp)…π(arene) interactions in the crystal structures of (31) and (32), leading to zero- and one-dimensional aggregation patterns in (a) and (b) respectively.

a solvent molecule, all four examples having Se(lp)···π(arene) interactions (33)–(36) (Figure 14.16) feature selenium in the +II oxidation state.

Compound (33), 3,4:7,8-bis(1,2-dicarba-closo-dodecaborano(1,2))-1,2,5,6-tetra-selenacyclo-octane toluene solvate [51], is a zero-dimensional aggregate whereby the centrosymmetric molecule, with the eight-membered [CSe$_2$C]$_2$ core being based on a chair, is connected to two solvent toluene molecules [d = 3.30 Å and θ = 0.5°] to form a three-molecular aggregate, as shown in Figure 14.17a. By contrast, when the same compound is recrystallised from benzene, which results in a non-symmetric, 1 : 1 solvate, a one-dimensional supramolecular chain is formed [52]. As shown in Figure 14.17b, the solvent benzene molecules provide almost equivalent Se(lp)···π(arene) links between the selenium(II) centres [d = 3.45 Å and θ = 13.3°; d = 3.46 Å and θ = 13.4°] to generate the chain.

Compounds (35) and (36) (Figure 14.16) are heterometallic and feature four and eight selenium(II) centres respectively. The molecular structure of the complex in (35), (tris(t-butylimido)tetraselane)-dichlorido-palladium benzonitrile solv-
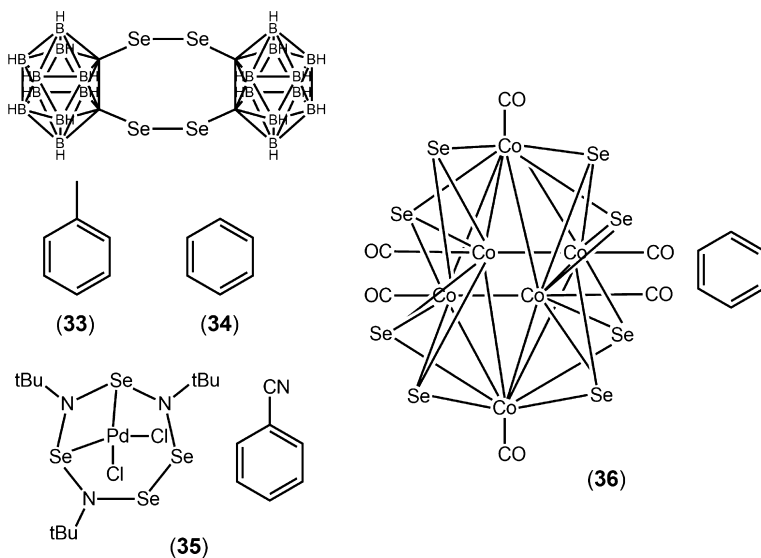
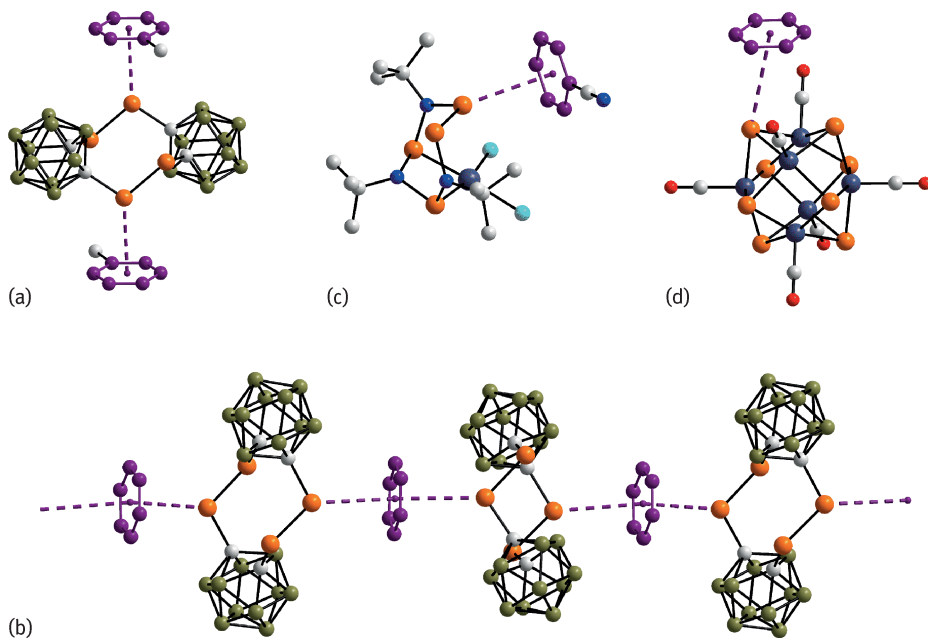**Fig. 14.16:** Chemical diagrams for (33)–(36).

Fig. 14.17: Supramolecular aggregation via Se(lp)...π(arene) interactions in the crystal structures of (33)–(36) shown in (a)–(d) respectively.

ate [53], features a buckled, seven-membered [SeNSe$_2$NSeN] ring with two selenium(II) atoms coordinated to a palladium atom. One of the non-coordinating selenium(II) atoms forms a Se(lp)···π(arene) interaction with the benzonitrile ring [d = 3.57 Å and θ = 14.4°] (Figure 14.17c). In the second heterometallic complex, octakis(μ_3-selenido)-hexacarbonyl-hexa-cobalt benzene solvate (36) [54], each face of the central Co$_6$ octahedron is capped by a selenium(II) atom. One of these selenium atoms is connected to the benzene ring via a Se(lp)···π(arene) interaction [d = 3.94 Å and θ = 15.8°] (Figure 14.17d).

14.3.4.2 Tellurium(II)

There is a sole example of a tellurium compound with a Te(lp)···π(arene) interaction between tellurium and a solvent molecule, namely (μ_3-1,4-ditelluridopertelluracyclohexane)-tris[(η^5-pentamethylcyclopentadienyl)rhenium(III,VII)] benzene solvate (37) [55] (see Marsh and Clemente [56] for a space group revision). In (37) (Figure 14.18), there are eight potential tellurium acceptors. It is one of the tellurium(II) atoms directly bound to a rhenium atom and not part of the Te$_6$ six-membered ring that forms the interaction [d = 3.75 Å and θ = 8.7°] (Figure 14.19).
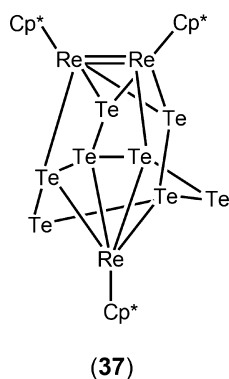

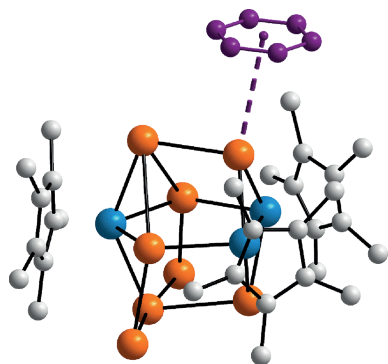**Fig. 14.18:** Chemical diagrams for (37). Cp* represents the η^5-pentamethylcyclopentadienyl anion.

Fig. 14.19: Supramolecular aggregation via a Te(lp)...π(arene) interaction in the crystal structure of (37).

14.4 Conclusions

In the foregoing sections, examples of main group element(lp)···π(arene) interactions have been described for elements in oxidation states, consistent with the presence of a lone-pair of electrons. These interactions usually lead to zero-dimensional aggregates with a few rare examples where, owing to the presence of bridging solvent, supramolecular chains are observed. The bonding description for element(lp)···π(arene) interactions is akin to that accepted for halogen bonding. The energies of these interactions are not high, as was shown in a recent computational chemistry study [38]. This suggests that the (gas phase) energy of attraction in the series of Menschutkin complexes, $SbCl_3$.benzene, $SbCl_3$.toluene (18) and $SbCl_3$.hexamethylbenzene, might vary systematically with increasing methyl substitution, i.e. 7.7, 8.5 and 15.5 kcal mol^{-1} respectively [38]. With this information in mind, it is apposite to recall the series of $BiCl_3$ structures (24)–(26), i.e. co-crystallised with similar solvents such as benzene, m-xylene and hexamethylbenzene. Increasing the methyl content in the rings resulted in very different supramolecular architectures; a result that may correlate with the energies of attraction between rings and steric effects. In summary, the experimental and theoretical studies both indicate that the insight offered by systematic study within this fascinating area of supramolecular chemistry will be significant.

Bibliography

[1] Zukerman-Schpector J, Haiduc I. Tellurium···π-aryl interactions: a new bonding motif for supramolecular self-assembly and crystal engineering. CrystEngComm, 2002, 4, 178–193.

[2] Haiduc I, Tiekink ERT, Zukerman-Schpector J. in Tin chemistry fundamentals, frontiers, and applications, ed. A. G. Davies, M. Gielen, K. H. Pannell and E. R. T. Tiekink, John Wiley & Sons Ltd., Chichester, 2008, p. 392–407.

[3] Tiekink ERT, Zukerman-Schpector J. Pb···π aryl interactions as supramolecular synthons. Aust. J. Chem. 2010, 63, 535–543.

[4] Caracelli I, Haiduc I, Zukerman-Schpector J, Tiekink ERT. M···π(arene) interactions for M = gallium, indium and thallium: influence upon supramolecular self-assembly and prevalence in some proteins. Coord. Chem. Rev. 2014, 281, 50–63.

[5] Zukerman-Schpector J, Otero-de la-Roza A, Luaña V, Tiekink ERT. Supramolecular architectures based on As(lone pair)···π(aryl) interactions. Chem. Commun. 2011, 47, 7608–7610.

[6] Caracelli I, Haiduc I, Zukerman-Schpector J, Tiekink ERT. Delocalised antimony(lone pair)- and bismuth-(lone pair)···π(arene) interactions: supramolecular assembly and other considerations. Coord. Chem. Rev. 2013, 257, 2863–2879.

[7]   Caracelli I, Zukerman-Schpector J, Tiekink ERT. Supramolecular aggregation patterns based on the bio-inspired Se(lone pair)···π(aryl) synthon. Coord. Chem. Rev. 2012, 256, 412–438.

[8]   Caracelli I, Haiduc I, Zukerman-Schpector J, Tiekink ERT, in The chemistry of organic selenium and tellurium compounds, ed. Z. Rappoport, John Wiley & Sons, Ltd, Chichester, 2013, vol. 4, p. 973–988.

[9]   Caracelli I, Zukerman-Schpector J, Haiduc I, Tiekink ERT. Main group metal lone-pair···π(arene) interactions: a new bonding mode for supramolecular associations. CrystEngComm. 2016, 18, 6960–6978.

[10] Caracelli I, Haiduc I, Zukerman-Schpector J, Tiekink ERT, in Aromatic interactions: frontiers in knowledge and application, eds D. W. Johnson and F. Hof, Royal Society of Chemistry, Abingdon, 2016, p. 98–123.

[11] Egli M, Sarkhel S. Lone pair-aromatic interactions: to stabilize or not to stabilize. Acc. Chem. Res. 2007, 40, 197–205.

[12] Jain A, Ramanathan V, Sankararamakrishnan R. Lone pair···pi interactions between water oxygens and aromatic residues: quantum chemical studies based on high-resolution protein structures and model compounds. Protein Sci. 2009, 18, 595–605.

[13] Cavallo G, Metrangolo P, Milani R, Pilati T, Priimagi A, Resnati G, Terraneo G. The halogen bond. Chem. Rev. 2016, 116, 2478–2601.

[14] Groom CR, Bruno IJ, Lightfoot MP, Ward SC. The Cambridge Structural Database. Acta Crystallogr. Sect. B: Struct. Sci. Cryst. Eng. Mat. 2016, 72, 171–179.

[15] Bruno IJ, Cole JC, Edgington PR, Kessler M, Macrae CF, McCabe P, Pearson J, Taylor R. New software for searching the Cambridge Structural Database and visualising crystal structures. Acta Crystallogr. Sect. B: Struct. Sci. 2002, 58, 389–397.

[16] Schollmeyer D, Shishkin OV, Rühl T, Vysotsky MO. OH–π and halogen–π interactions as driving forces in the crystal organisations of tri-bromo and tri-iodo trityl alcohols. CrystEngComm, 2008, 10, 715–723.

[17] Spek AL. Single-crystal structure validation with the program PLATON. J. Appl. Crystallogr. 2003, 36, 7–13.

[18] DIAMOND, Visual crystal structure information system, version 3.1. CRYSTAL IMPACT, Bonn, Germany, 2006.

[19] Fillebeen T, Hascall T, Parkin G. Bis- and tris(pyrazolyl)hydroborato ligands with bulky triptycyl substituents: the synthesis and structural characterization of Tl[BpTrip] and Tl[TpTrip]. Inorg. Chem. 1997, 36, 3787–3790.

[20] Yap GPA, Jove F, Urbano J, Alvarez E, Trofimenko S, Diaz-Requejo MM, Perez PJ. Unusual polybrominated polypyrazolylborates and their copper(I) complexes: synthesis, characterization, and catalytic activity. Inorg. Chem. 2007, 46, 780–787.

[21] Yi R, Palmer JH, Parkin G. Benzannulated tris(2-mercapto-1-imidazolyl)hydroborato ligands: tetradentate κ^4-S_3H binding and access to monomeric monovalent thallium in an [S_3] coordination environment. Dalton Trans. 2014, 43, 1397–1407.

[22] Schmidbaur H, Bublak W, Riede J, Muller G. [{1,3,5-$(CH_3)_3H_3C_6$}$_6$Tl$_4$][GaBr$_4$]$_4$ – synthesis and structure of a mixed mono- and bis(arene)thallium complex. Angew. Chem. Int. Ed. 1985, 24, 414–415.

[23] Harvey S, Lappert MF, Raston CL, Skelton BW, Srivastava G, White AH. Conversion of the silicone poly(dimethylsiloxane) by thallium(I) ethoxide into the ladder polymer [{Tl$_2$(OSiMe$_2$)O}$_2$]$_n$; X-ray structure of the product and of thallium(I) triphenylsilanolate. Chem. Commun. 1988, 1216–1217.

[24] Hellmann KW, Gade LH, Fleischer R, Kottke T. Aggregation, reaggregation and degradation of a trifunctional thallium(I) amide induced by weak Tl$^{I···}$Tl^I attraction. Chem. Eur. J. 1997, 3, 1801–1806.

[25] Boyle TJ, Doan TQ, Steele LAM, Apblett C, Hoppe SM, Hawthorne K, Kalinich RM, Sigmund WM. Tin(II) amide/alkoxide coordination compounds for production of Sn-based nanowires for lithium ion battery anode materials. Dalton Trans. 2012, 41, 9349–9364.

[26] Hosmane NS, Zhang H, Maguire JA, Demissie T, Oki AR, Saxena A, Lipscomb WN. New stanna- and plumba-carboranes: synthetic and structural investigation. Main Group Met. Chem. 2001, 24, 589–596.

[27] Birchall T, Johnson JP. Crystal structure of di-μ3-oxo-octakis-μ-(trifluoroacetato)-ditin(II) ditin(IV)−benzene (1/1). J. Chem. Soc., Dalton Trans. 1981, 69–73.

[28] Tam ECY, Coles MP, Smith JD, Fulton JR. The steric influence of β-diketiminato ligands on the coordination chemistry of lead(II). Polyhedron. 2015, 85, 284–294.

[29] Ranis LG, Werellapatha K, Pietrini NJ, Bunker BA, Brown SN. Metal and ligand effects on bonding in Group 6 complexes of redox-active amidodiphenoxides. Inorg. Chem. 2014, 53, 10203–10216.

[30] Hosmane NS, Siriwardane U, Hong Zhu, Zhang G, Maguire JA. The first structural evidence for the insertion of an unsubstituted lead into a carborane cage. Organometallics, 1989, 8, 566–568.

[31] Edelmann FT, Buijink J-KF, Brooker SA, Herbst-Irmer R, Kilimann U, Bohnen FM. Formation and structure of the oxygen-centered lead thiolate cluster $Pb_5O(SR_F)_8 \cdot 2 C_7H_8$ [R_F = 2,4,6-Tris(trifluoromethyl)phenyl]. Inorg. Chem. 2000, 39, 6134–6135.

[32] Gash AG, Rodesiler PF, Amma EL. Metal ion-aromatic complexes. XV. Synthesis, structure, and bonding of $\pi\text{-}C_6H_6Pb(AlCl_4)_2 \cdot C_6H$. Inorg. Chem. 1974, 13, 2429–2434.

[33] Schmidbaur H, Nowak R, Steigelmann O, Muller G. π-Complexes of p-block elements: synthesis and structures of adducts of arsenic and antimony halides with alkylated benzenes. Chem. Ber. 1990, 123, 1221–1226

[34] Shang S, Khasnis DV, Zhang H, Small AC, Fan M, Lattman M. Insertion of one and two Arsenic atoms into calix[4]arenes. Inorg. Chem. 1995, 34, 3610–3615.

[35] Stubenhofer M, Kuntz C, Balazs G, Zabel M, Scheer M. 1,2,3-Triphosphole derivatives as reactive intermediates. Chem. Commun. 2009, 1745–1747.

[36] Schier A, Wallis JM, Müller G, Schmidbaur H. $[C_6H_3(CH_3)_3][BiCl_3]$ and $[C_6(CH_3)_6][BiCl_3]_2$, arene complexes of bismuth with half-sandwich and "inverted" sandwich structures. Angew. Chem., Int. Ed. Engl., 1986, 25, 757–759.

[37] Schmidbaur H, Schier A. π-Complexation of post-transition metals by neutral aromatic hydrocarbons: the road from observations in the 19th century to new aspects of supramolecular chemistry. Organometallics 2008, 27, 2361–2395.

[38] Lo R, Svec P, Ruzickova Z, Ruzicka A, Hobza P. On the nature of the stabilisation of the E···π pnicogen bond in the $SbCl_3$···toluene complex. Chem. Commun. 2016, 52, 3500–3503.

[39] Schmidbaur H, Wallis JM, Nowak R, Huber B, Muller G. Aromaten-Komplexe mit Halbsandwich-Struktur: Die 1:1-komplexe des mesitylens mit $SbCl_3$, $SbBr_3$, $BiCl_3$ und $BiBr_3$. Chem. Ber. 1987, 120, 1837–1843.

[40] Mootz D, Handler V. Crystal structure of the Menshutkin complex benzene · 2 $SbCl_3$. Z. Anorg. Allg. Chem. 1986, 533, 23–29.

[41] Hulme R, Mullen DJE. Crystal structure of the 2:1 antimony trichloride: p-xylene intermolecular compound at −110 ºC. J. Chem. Soc. Dalton Trans. 1976, 802–804.

[42] Kishore PVVN, Baskar V. Hexa- and trinuclear organoantimony oxo clusters stabilized by organosilanols. Inorg. Chem. 2014, 53, 6737–6742.

[43] Ly HV, Parvez M, Roesler R. An unusual ligand in copper chemistry: coordination oligomers and polymers containing the $[\{CpMo(CO)_2\}_2(\mu, \eta^2\text{-}Sb_2)]$ cluster. Inorg. Chem. 2006, 45, 345–351.

[44] Breunig HJ, Lork E, Rat C. The complex $BiCl_3 \cdot CH_3C_6H_5$. Z. Naturforsch., B: Chem. Sci. 2007, 62, 1224–1226.

[45] Muller-Becker S, Frank W, Schneider J. Schwermetall-π-Komplexe. IX. Die kettenpolymere $[(1,2-(CH_3)_2C_6H_4BiCl_3)_2]$, $[(1,3)(CH_3)_2C_6H_4BiCl_3)_2]$ und $[(1,4-(CH_3)_2C_6H_4BiCl_3)_2]$. Z. Anorg. Allg. Chem. 1993, 619, 1073–1082.

[46] Andrews PC, Junk PC, Nuzhnaya I, Spiccia L. Fluorinated bismuth alkoxides: from monomers to polymers and oxo-clusters. Dalton Trans. 2008, 2557–2568.

[47] Sharutin VV, Egorova IV, Sharutina OK, Ivanenko TK, Adonin NY, Starichenko VF, Pushilin MA, Gerasimenko AV. Tetranuclear bismuth complexes $Bi_4(O)_2(O_2CC_6H_2F_3-3,4,5)_8.2\,C_6H_6$ and $Bi_4(O)_2(O_2CC_6H_2F_3-3,4,5)_8.2\,C_6H_4Me_2-1,4$: synthesis and structures. Russ. J. Coord. Chem. 2005, 31, 2–8.

[48] Sharutin VV, Egorova IV, Sharutina OK, Ivanenko TK, Adonin NY, Starichenko VF, Pushilin MA, Gerasimenko AV. Tetranuclear bismuth complex $Bi_4(O)_2(O_2CC_6H_2F_3-3,4,5,)_8 \cdot 2\eta^6\text{-}C_6H_5Me$: synthesis and structure. Russ. J. Coord. Chem. 2003, 29, 838–844.

[49] Liu L, Zakharov LN, Rheingold AL, Hanna TA. Synthesis and X-ray crystal structures of the first antimony and bismuth calixarene complexes. Chem. Commun. 2004, 1472–1473.

[50] Mehring M, Schurmann M. The first bismuth phosphonate cluster. X-ray single crystal structure of $[(Bu^tPO_3)_{10}(Bu^tPO_3H)_2Bi_{14}O_{10} \cdot 3\,C_6H_6 \cdot 4\,H_2O]$. Chem. Commun. 2001, 2354–2355.

[51] Wrackmeyer B, Hernandez ZG, Kempe R, Herberhold M. Novel 1,2-Dicarba-closo-dodecaborane(12) derivatives of selenium. Eur. J. Inorg. Chem. 2007, 239–246.

[52] Garcia-Hernandez Z, Wrackmeyer B, Herberhold M. Irrgang T, Kempe R. Crystal structure of 3,4,7,8-bis(l,2-dicarba-closo-dodecaborano[l,2])-1,2,5,6-tetraselenacyclooctane benzene solvate, $[(C_2Bi_{10}H_{10})Se_2]_2.C_6D_6$. Z. Kristallogr. New Cryst. Struct. 2006, 221, 419–420.

[53] Risto M, Eironen A, Mannisto E, Oilunkaniemi R, Laitinen RS, Chivers T. Palladium complexes containing novel cyclic selenium imides. Dalton Trans. 2009, 8473–8475.

[54] Gervasio G, Kettle SFA, Musso F, Rossetti R, Stanghellini PL. Synthesis and characterization of three novel selenidohexacobalt carbonyl clusters. Crystal structures of $[(\mu_3\text{-}Se)Co_3(CO)_7]_2\mu_4\text{-}(Se_2)$ and $Co_6(\mu_3\text{-}Se)_8(Co)_6 \cdot 2\,C_6H_6$. Inorg. Chem. 1995, 34, 298–305.

[55] Jin G-X, Arikawa Y, Tatsumi K. Spontaneous formation of a diamond-crown structure of Re_8 polyselenide and a cage structure of Re_3 polytelluride. J. Am. Chem. Soc. 2001, 123, 735–736.

[56] Marsh RE, Clemente DA. A survey of crystal structures published in the Journal of the American Chemical Society. Inorg. Chim. Acta. 2007, 360, 4017–4024.